Introduction

In recent years, Unmanned Aerial Vehicles (UAVs) have become of widespread use in both military and commercial domains. There are two dominant types of UAVs - (1) multi-rotor UAVs, which have high manoeuvrability and accessibility, especially in terms of take-off and landing, and (2) fixed-wing variety UAVs, of which the main advantages lie in their generally longer flight time and range capabilities (Boon et al. 2017). In the military scene, these benefits mean that fixed-wing UAVs are vastly more popular, taking up 97% of the military market (Cai et al., 2014). Yet the difficulty that comes with manoeuvrability of such fixed-wing UAVs, particularly in landing, has made the rotary variety more popular commercially.

This study explores methods to marry the benefits of fixed-wing UAVs with the unique ability to land and retrieve such fixed-wing UAVs in an urban setting where the available landing space can be tight. This could allow UAVs to land within dense regions of buildings, or even into buildings, which when combined with currently-researched perch landing methods, allows for operations into foreigh territory. Fixed-wing UAVs, which do not have the same vertical take-off and landing (VTOL) capabilities as multi-rotor UAVs, conventionally struggle to land in such settings.

Specifically, we seek to explore the use of fixed-wing stall to land a UAV within a predictable target region. The issue of stalling, or the sudden loss of lift and increase of drag experienced by aircraft as a result of a steep Angle of Attack(AoA), is one that plagues aircrafts as a hazard during take-off and landing. However, in the landing procedures of fixed-wing UAVs, where the increased g-forces caused by sudden deceleration are not a concern due to the lack of human passengers, this sudden increase in drag caused by stall can be used to our advantage to land within small and confined regions. By making use of stall, we can quickly reduce horizontal velocity and land or travel to the specified region – additionally, as this method is purely algorithmic, it does not require additional devices to be attached to the UAV, increasing the potential payload of the UAV.

In this report, we outline and document our progress in the formulation of a control algorithm to trigger stall landing in a simulated environment.

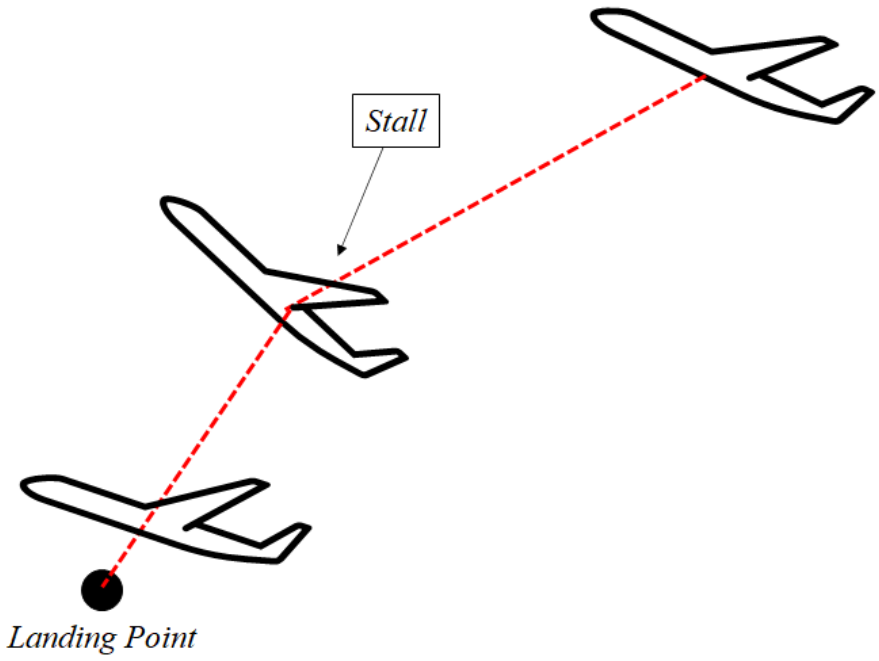

Fig1.1: Our targeted flight path

Literature Review

This section highlights earlier research covering various methods to land a fixed-wing UAV.

Wyllie, T. (2001) described various parachute landing mechanisms that allow for controlled and safe landing of UAVs with relative ease and simplicity. However, the paper described an accuracy trade-off, particularly in high wind situations, where the landing point is difficult to predict, and there is much less control over the landing.

Methods involving landing on mobile ground vehicles (T. Muskardin et al., 2016) and landing inside of nets (H. J. Kim et al., 2013) have been described also, but such landing methods require a pre-setup landing spot, which in many military applications, is not available to the users of the UAV. Hence, our stall landing method provides a needed alternative to landing in a undeveloped area with little available room.

Hybrid UAVs, which are fixed-wing UAVs that feature VTOL capabilities by transformable wings, have been proposed as a solution to this, but these UAVs are much more complex, increasing cost and decreasing potential payload. (Saeed et al., 2018)

In terms of using stall landing methods to land fixed-wing UAVs, Tanigutchi (2008) proposed and simulated the deep stall landing of a free flight aircraft in the longitudinal plane, using wind tunnel data for a NACA 0012 airfoil. It stated that "the only mechanism to get the plane into deep stall is to quickly tilt the horizontal tail plane", and explained how this deep stall allowed for a decrease in the speed of the plane. The paper analysed the ability of the aircraft to stabilise at a final trim state, and validated its simulation using physical testing.

Park S. (2020) also analysed a similar problem, but employed a more sophisticated blade element theory to find forces on the aircraft and designed a flight path controller for 3 dimensions. The analysis was verified with experimental results like in Tanigutchi (2008).

Mathisen et al. (2015) created a non-linear predictive control for deep stall landing, which was needed as "the non-linearities and constraints in the model demands a more flexible controller than linear controllers". They then tested the control algorithm in a simulation with randomly varying wind conditions, showing that the landing accuracy of their algorithm was acceptable at winds up to 7ms-1.

In addition, a stall-based method of "perching and resting" inspired by the perching of birds in nature, which allows the UAV to take-off again from its landing point, was proposed and investigated by Crowther W.(2000). In the landing procedure proposed by Drowther, the airplane, travelling horizontally to the ground, pitches up, gaining altitude, before stalling and landing at that higher altitude in a perched position. Hang et al. (2019) featured development of the landing gear for such a perching method, showing how it would be practical for landing on many surfaces and saving power. The reduction of speed before such a landing is crucial, and stalls were used as part of the landing procedure.

The stall itself has also been researched in the context of identification and prevention, as deep stall, where a plane is unable to recover from a stall condition, is a danger to airplanes during take-off and landing. White and Cooper (1965) first identified the potential risks of the deep stall condition, defined as a condition beyond initial stall that is difficult to recover from. Kolb et al. (2019) investigated the detection and prevention of aircraft deep stall to avoid going into deep stall during take-off and landing. The primary cause for this phenomenon was stated in both papers as the "flight

of the T-tail [being] inside the separated wake of the stalled main wing", causing the plane to be trapped in a state of stall.

Methodology

The approaches adopted by Tanigutchi, Park S., Siri H. et al. and Mathisen et al. included the characterisation of existing aircraft designs to predict the aerodynamic forces at play throughout the landing. Similarly, we aimed to characterise the stall characteristics of a UAV model, for the formulation and testing of our proposed flight path control logic in a simulated environment.

Characterisation Phase

Initially, we had considered making use of XFLR5 to obtain lift and drag coefficient data for the stall. However, due to the invicid fluid assumption of XFLR5 and its failure to resolve airflow accurately in the post-stall state, we turned to CFD RANS simulations instead.

In the characterisation phase, we first defined a model for our UAV and then used Ansys CFX to find lift and drag values at different AoAs and velocities. This was done separately on the elevator, such that its contribution to lift could be modelled independently in the future simulation phase.

Defining the UAV

We based our UAV model design on the existing design specifications of the RQ-11 Raven manufactured by AeroVironment.

In our simulation, the UAV was modelled as a hollow aluminium rod, with a wing attached 0.1m from the front, and an elevator and tail at the end. A NACA 2412 airfoil was used for both the wing and elevator. We modelled the main wing and the aluminium rod attached together for their drag performance but took the aluminium rod's lift contribution to be minimal.

The dimensions for all these components are included in the tables below:

Rod

Parameter	Length (m)
Outer Radius	0.04
Inner Radius	0.025
Length	0.9

Main Wing (NACA 2412)

Parameter	Length (m)
Wingspan	1.4
Chord Length Volume = 0.00616m	0.22

Elevator (NACA 2412)

Parameter	Length (m)
Wingspan	0.4
Chord Length	0.12

The above parameters were used to initialise separate CAD models for the rod + main wing + tail, and the elevator respectively, and an air boundary that leaves 0.1m above and below the wing when it is rotated was defined. This allowed for adequate space for the airflow, even as we turned the wing towards higher angles, while keeping the processing time of the simulation minimal.

The test was run in Ansys CFX as a wind tunnel test, with a k-epsilon SST turbulence model and the total force in the Y+ and Z+ directions was taken as lift and drag respectively. The boundary condition of the walls was left as non-sticking walls, and the airfoil surface is treated as a sticking surface. The front and back walls of the air boundary were defined as inlet and outlet with set wind velocity and dependent pressure respectively.

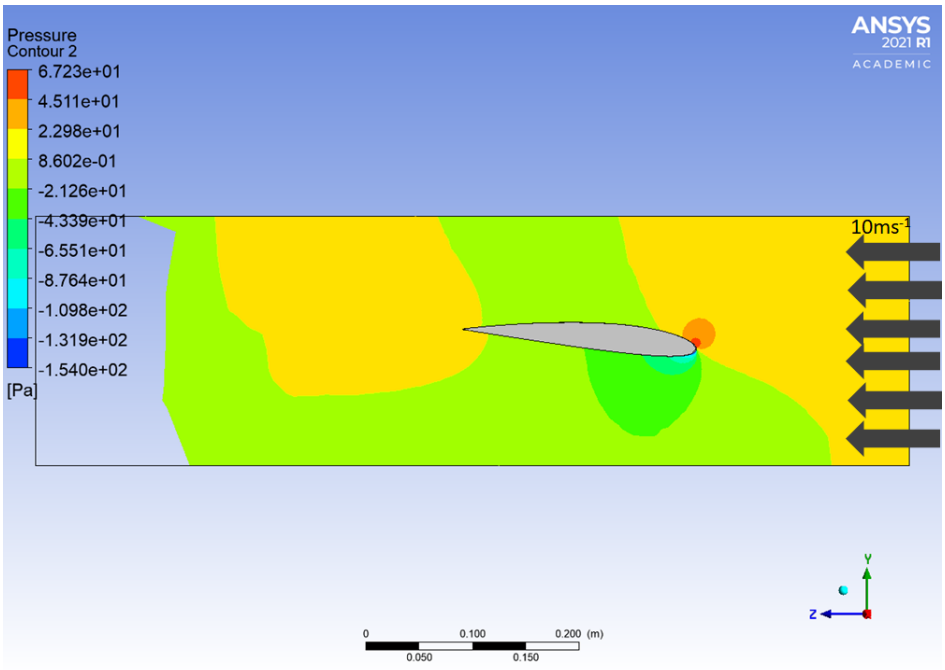

Fig 4.1: A Sample of the pressure gradient of a wing at 10° AoA and 10ms-1 upwind

Lift and Drag forces were set as output parameters, and multiple runs with the discretely varying parameters of AoA and inlet wind velocity from –70° to 80° and 10ms-1 to 25ms-1 respectively are intended to be computed, but due to the computation-heavy nature of this, they have not yet completed running at the present moment. Here two of the graphs (Graphs 4.1, 4.2) attained thus far, of lift and drag of our main wing at 10ms-1 upwind, as a proof-of-concept:

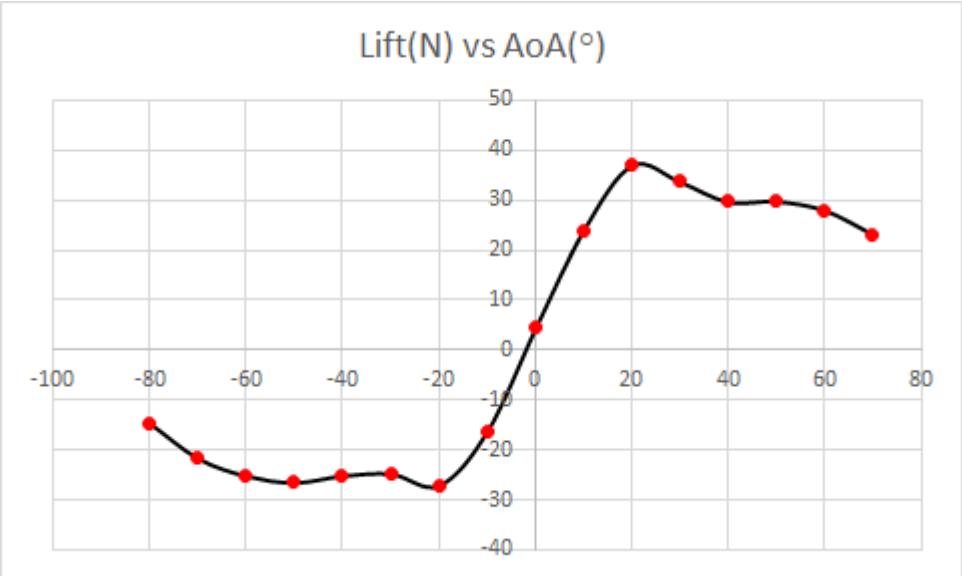

Graph 4.1: Lift vs AoA graph for 10ms-1 upwind

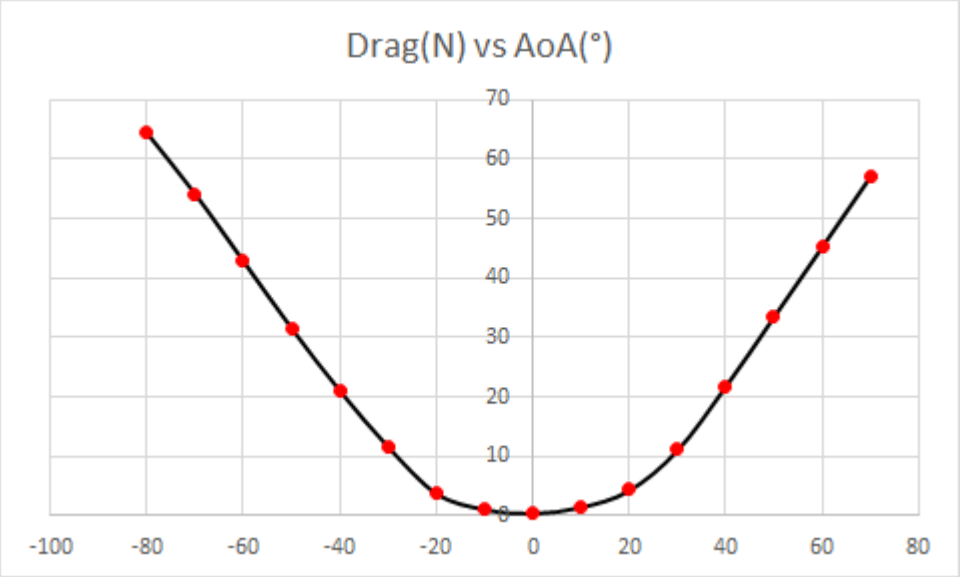

Graph 4.2: Drag vs AoA graph for 10ms-1 upwind

Comparison to an XFLR5 NACA2412 Result

We compared the obtained lift graph with one obtained from XFLR5 of a similar 2412 airfoil. As can be seen, the general shape of the graph is similar, however, the XFLR5 model underpredicts the stall angle, or the positive angle where the graph begins to decline, to be 15 degrees, while our data predicted it to be closer to 20 degrees.

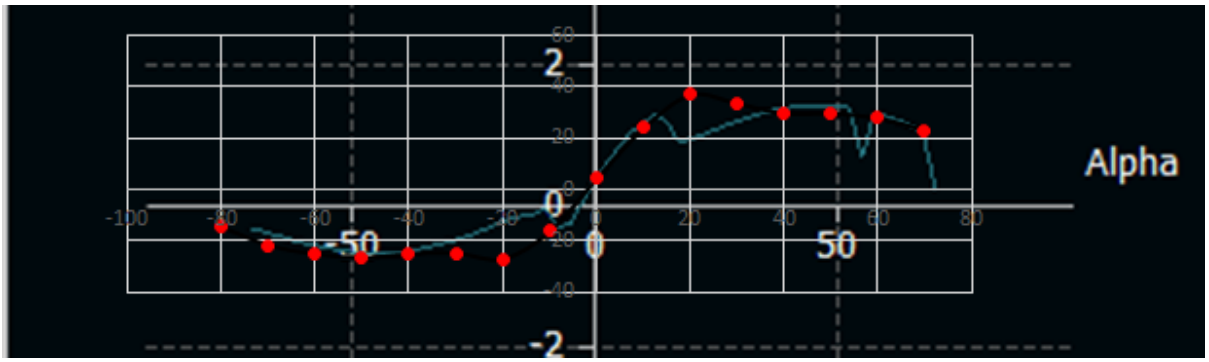

This approximate angle of 20 degrees as a stall angle agrees with other simulator studies of the NACA 2412 airfoil. (Velkova et al., 2016)

Upon completing the resource-heavy simulation of the system at different AoAs and wind speeds, the data can then be extrapolated to find the lift and drag forces acting on the plane's wings at each point, given its direction and speed(giving a relative wind).

Next Steps

The ultimate aim of this simulation is to find a set of controls that will allow this fixed-wing UAV to glide downwards, towards a specified landing spot, in a straight path. During this decline, a stall will be triggered by a sudden tilt of the elevator, reducing the horizontal velocity of the UAV,

Unfortunately, due to the computation-heavy nature of the second step (separate remeshing and CFD simulations must be run for all angles between –70 and 80, and this must be repeated for the range of wind velocities we want to use, and this must be done for both the aerodynamic body of the plane, as well as the elevator flaps), the data from this step is unable to be completed as of now, 29th May 2021.

Upon receiving the lift and drag datasets, we can use these characterised values to run simulations in a python environment, which allows for calculation of the plane's movement by timestep. The python environment will be initialised as such:

1. The plane is defined by a set of 6 vectors:

Position, Velocity, Acceleration, Rotational Position, Angular Velocity, Angular Acceleration

For simplicity, whilst we are using forces for a 3D wing so as to take into account vortex effects at the wing tip, we restrict the aircraft to 2D motion.

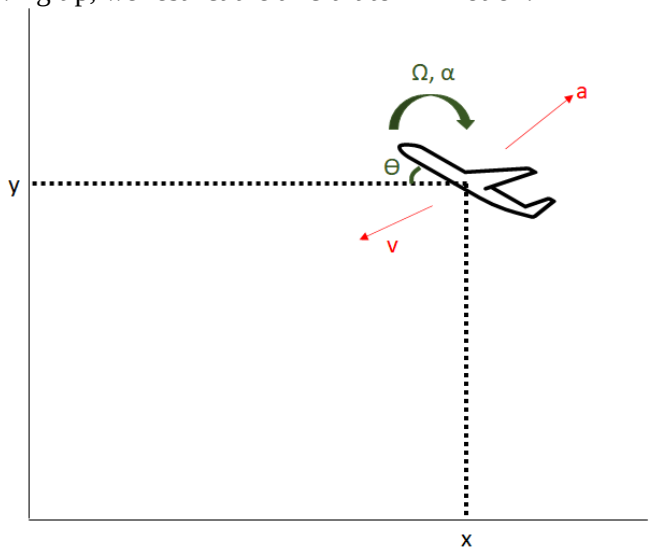

Fig 4.2: The parameters of our simulation - Θ, Ω, α refer to rotational rosition, angular velocity, angular acceleration respectively, and x, y, v_x , v_y , a_x ,a_y refer to position, velocity and acceleration in 2 directions respectively

2. At each timestep, we can find the total lift and drag force acting on the plane based on the forces attained from the plane body, as well as the added contribution of the elevator flap which is defined and controlled at the timestep. This step uses the current Θ and velocity of the plane to find AoA and relative wind.
3. Using the forces calculated in step 2, we find the acceleration, both translational and rotational.
4. We find values for new velocity and position, and repeat across all time steps.

By controlling the elevator, we change the acceleration calculated in step 2, which changes the velocity and goes on to affect the position in a later timestep.

Ideally, we would like to minimise the landing time as well, for a given maximum landing impulse, and this can be achieved using an evolutionary computing algorithm. This method is proposed as further work.

Citations

Boon, M. A., Drijfhout, A. P., & Tesfamichael, S. (2017). COMPARISON OF A FIXED-WING AND MULTI-ROTOR UAV FOR ENVIRONMENTAL MAPPING APPLICATIONS: A CASE STUDY. ISPRS - International Archives of the Photogrammetry, Remote Sensing and Spatial Information Sciences, XLII-2/W6, 47–54. https://doi.org/10.5194/isprs-archives-xlii-2-w6-47-2017

Cai, G., Dias, J., & Seneviratne, L. (2014). A Survey of Small-Scale Unmanned Aerial Vehicles: Recent Advances and Future Development Trends. Unmanned Systems, 02(02), 175–199. https://doi.org/10.1142/s2301385014300017

Wyllie, T. (2001), "Parachute recovery for UAV systems", Aircraft Engineering and Aerospace Technology, Vol. 73 No. 6, pp. 542-551. https://doi.org/10.1108/00022660110696696

T. Muskardin, G. Balmer, S. Wlach, K. Kondak, M. Laiacker and A. Ollero, "Landing of a fixed-wing UAV on a mobile ground vehicle," 2016 IEEE International Conference on Robotics and Automation (ICRA), 2016, pp. 1237-1242, doi: 10.1109/ICRA.2016.7487254.

H. J. Kim et al., "Fully Autonomous Vision-Based Net-Recovery Landing System for a Fixed-Wing UAV," in IEEE/ASME Transactions on Mechatronics, vol. 18, no. 4, pp. 1320-1333, Aug. 2013, doi: 10.1109/TMECH.2013.2247411.

Crowther, W. (2000). Perched Landing and Takeoff for fixed wing UAV\'s. In Symposium on Unmanned Vehicles for Aerial, Ground and Naval Military Operations, Conference Location: Ankara, Turkey

Hang, Kaiyu & Ximin, Lyu & Song, Haoran & Stork, Johannes & Dollar, Aaron & Kragic, Danica & Zhang, Fu. (2019). Perching and resting—A paradigm for UAV maneuvering with modularized landing gears. Science Robotics. 4. eaau6637. 10.1126/scirobotics.aau6637.

Saeed, A. S., Younes, A. B., Cai, C., & Cai, G. (2018). A survey of hybrid Unmanned Aerial Vehicles. Progress in Aerospace Sciences, 98, 91–105. https://doi.org/10.1016/j.paerosci.2018.03.007

H. Taniguchi, “Analysis of deepstall landing for UAV,” vol. 3, pp. 2498–2503, 2008

Park, S. (2020). Control and Guidance for Precision Deep Stall Landing. Journal of Guidance, Control, and Dynamics, 43(2), 365–372. https://doi.org/10.2514/1.g004058

Mathisen, S. H., Fossen, T. I., & Johansen, T. A. (2015). Non-linear model predictive control for guidance of a fixed-wing UAV in precision deep stall landing. 2015 International Conference on Unmanned Aircraft Systems (ICUAS). https://doi.org/10.1109/icuas.2015.7152310

Cooper, George & White, Maurice. (1965). Simulator Studies of the Deep Stall.

Kolb, Sébastien & Montagnier, Olivier & Hétru, Laurent & Faure, Thierry. (2019). Real-Time Detection of an Aircraft Deep Stall and Recovery Procedure. Journal of Guidance, Control, and Dynamics. 42. 1-10. 10.2514/1.G003729.

Velkova, Cvetelina & Branger, Terence & Calderon, Francesco & Soulier, Camille. (2016). THE IMPACT OF DIFFERENT TURBULENCE MODELS AT ANSYS FLUENT OVER THE AERODYNAMIC CHARACTERISTICS OF ULTRA-LIGHT WING AIRFOIL NACA 2412.